Experimental Slip Measurement of Roller Bearings

Sahar Mirzaei[1], Thomas Fahlbusch [1],Eduard Reithmeier [1]
[1]Institute for Measurement and Control Engineering, Leibniz Universität Hannover
Nienburger Straße. 17, 30167 Hannover, Germany
Email: Sahar.mirzaei@imr.uni-hannover.de

Abstract
The knowledge, on which operating conditions a cylindrical roller bearing not only rotates but also slides, is very important to avoid early bearing failure. In this paper the roller slippage of a cylindrical roller bearing under certain operation conditions is experimentally examined. For measuring the slip a new optical Method, the Derotator-technique, is applied. In combination with digital image processing techniques, the movement of single roller elements are analyzed. Thereby, the exact sliding behaviour is measured.

Keywords:
Roller bearings, Slip measurement, Derotator

1 INTRODUCTION

Under ideal conditions a rolling bearing should act as a planetary system with pure rolling condition at its surfaces. If the radial load on a cylindrical roller bearing is not high enough to develop a frictional drive force between the rolling elements and the rotating raceways to overcome drag, slippage will occur. With the slippage S the sliding movement between the rolling elements will be described. It is a specific value that describes the relative difference between the measured angular speed $n_{mes.}$ and the theoretical angular speed $n_{theor.}$ under ideal rolling conditions of a bearing.

$$S = \frac{n_{theor.} - n_{meas.}}{n_{theor.}} \quad (1)$$

From experimental examinations and technical applications the occurrence of non-stationary slip, especially in cylindrical roller bearings, can be implicated with the occurrence of smearing. For example during operation of cylindrical roller bearings under low radial load and high shaft speed, skidding, i.e. considerable cage and roller slip can cause excessive wear and failure of the bearing inner ring and it's roller surface. This leads to a minor service life of the bearing. This failure is called "skidding damage". The knowledge, under which operational conditions cage slip and rolling element slip occur is of importance to estimate the correct run behaviour of the bearing under certain conditions. Slip in a roller bearing does not necessarily cause wear at all load and operation conditions [1]. Therefore, it is required to measure and monitor the slip behaviour of the bearing during its service. Numerous experimental and theoretical analysis about roller slip in bearings and measurement techniques of slip are carried out up to now [1-9]. In most cases the measurement methods are either for big sized bearings or they are to complex for industrial applications [1, 2].

In this paper a new optical method for the measurement of roller slippage is presented. In this method an image derotator and a high speed camera are applied to observe the bearing during operation. Furthermore, digital image processing techniques are used to determine the roller angular speed and to calculate the roller slip.

This paper is organized as follows: section 2 gives a brief review of the functional behaviour of the image derotator. In section 3 the experimental setup and procedures are introduced. The digital image processing algorithms in this work is explained in section 4. Section 5 discusses the results of the experimental examinations. Afterwards, a brief summary will be given in section 6.

2 PRINCIPAL OF THE IMAGE DEROTATOR

For measuring the roller slip, an optical measurement system named "derotator" is applied. The main component of the derotator is a Dove-Prism. If a rotary object will be monitored through this prism, which rotates with the half of the rotational speed of the object, the object will appear in a stationary view. Therefore the optical axis of the prism, the rotary axis of its drive and the object rotary axis must be identical. Figure 1 shows the optical path by two different rotation angles of the prism. In this case the simulation of a single point of the object is shown. In the first image the prism and object are located at the zero position. In the second figure the object is located at the position $\varphi = 80°$. The prism is located at $\varphi = 40°$. Thereby, the image of the object does not move any more [14].

The derotator exhibits a gimbal-mounted adjusting unit whereby the derotator's rotational axis can be manipulated individually to the object's rotational axis. The synchronization of the rotational speed of the derotator and the object amounts a ratio of 2:1. This motion behaviour is realized by a real time cascade control with Matlab xPC Target. The maximum rotation speed of the object is n_{max}= 10.000 U/min.

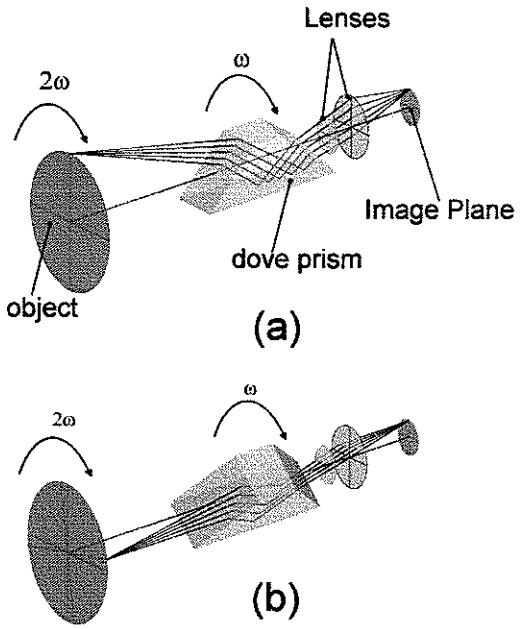

Figure 1: Optical path through the dove prism for two different rotation angles (a) object rotation angle 2ω = 0° (b) object rotation angle 2ω = 80°

3 EXPERIMENTAL

3.1 Experimental setup

The setup used in these investigations is shown in Figure 2. It consists of a bearing setup, an image derotator and a high speed camera.

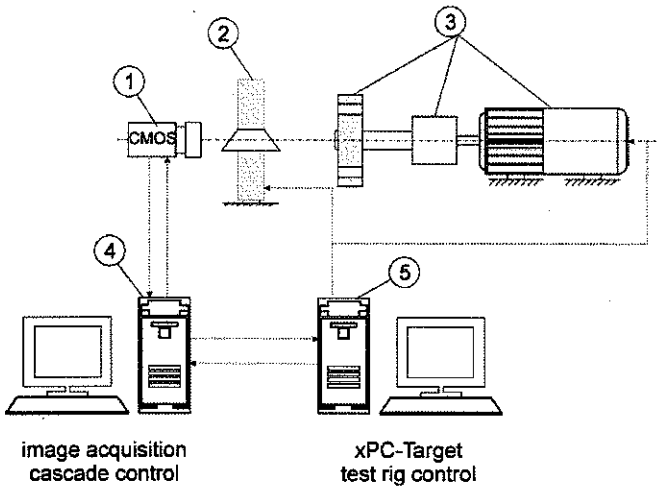

Figure 2: Schematic view of the test rig. 1) high speed camera, 2) image derotator, 3) bearing set up 4) image acquisition and host PC for control calculation 5) XPC-Target for control implementation

The high speed camera is a CMOS-Camera with a recording frequency of f = 500 images/s at a maximum resolution of 1280 x 1024 pixels. For the transmission of the data a frame grabber card with "camera Link" is applied. The control of the derotator's angular speed is processed under xPC Target. xPC Target is a tool for rapid implementation of real-time control systems on a digital computer. The software works through MATLAB Simulink, allowing a control system to be designed in block diagram form in Simulink and then to be realized in the physical world with no need for any low-level programming or circuit assembly. The block diagram is compiled to an executable and then loaded onto a dedicated computer (Target PC) for real-time execution. The Target PC contains the computer hardware that executes the controller. This means that the entire machine is dedicated to do nothing but running the controller program. The bearing setup is shown in Figure 3.

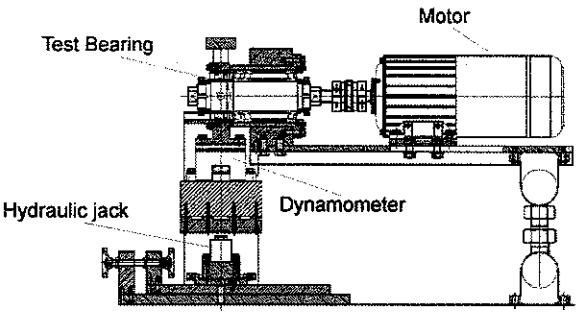

Figure 3: Bearing setup

The shaft and test bearing are driven by a DC motor with continuous rotational frequency. The radial load of the bearing is applied by a hydraulic lift jack. The outer ring of the test bearing is placed in the mounting, which is placed directly on a dynamometer.

3.2 Test bearing

The test bearing is a SKF NU 216 ECP bearing with having a bore, outer diameter and width of 80 mm x 125 mm x 22 mm, respectively. The bearing has a glass fibre reinforced polyamide cage, containing 18 rollers. The basic dynamic load of this bearing is about F = 66 kN.

3.3 Experimental conditions and procedures

The shaft is driven with the rotational speed n_s = 200 - 1000 ± 10 rpm. The radial load is determined from the minimum load equation of SKF:

$$F_{rm} = k_r \left(6 + \frac{4n_s}{n_r}\right)\left(\frac{d_m}{100}\right)^2 \qquad (2)$$

with:

F_{rm} = minimum radial load, kN

k_r = minimum load factor = 0.15

n_s = shafts rotational speed, rpm

n_r = reference speed, rpm = 6300 rpm

d_m = bearing mean diameter

$d_m = 0.5(d + D)$ = 102.5 mm

One of the rollers is marked on it's surface three times. In this experiment the derotator is rotating with half of the rotational speed of the bearing cage n_c. So the rotational movement of the cage and the roller around the inner ring will be eliminated. Thereby the examination of the rotational speed of the roller around its axis is possible. With the high speed camera the sequential images of the bearing during operation is captured with a frame rate of f = 700 Hz and resolution of 761 x 720 Pixel. By tracking the three markers on the roller surface and calculating the distance that one marker covers between two frames,

the roller rotational speed is determined. For tracking these markers, digital image processing algorithms are used. These algorithms will be described in the following section.

4 DIGITAL IMAGE PROCESSING ALGORITHMUS

For the tracking procedure of the markers on the roller in sequential images, the desired roller is firstly chosen in the images. Afterwards a circle is fitted on the roller. For fitting the circle, the Hough transform algorithm is used.

In the original Hough transform method for finding circles [11], firstly the intensity gradient of the gray level image is estimated. Then it is thresholded to give the position of the significant edges. Afterwards for each radius of the circle that is to be detected a separate circle filter can be used:

$$(x-x_c)^2-(y-y_c)^2=R^2 \tag{3}$$

For every edge pixel (x,y) the position of the possible centre location (x_c,y_c) in a distance R will be accumulated in parameter space. This forms a three dimensional parameter space, where two dimensions represent the position of the circle centre and the third its radius size. Finally, the parameter space will be scanned for maximum peaks that correspond to the centre of the circle with the searched radius [10].

Since this approach needs a large number of points be accumulated in parameter space, a revised form of this method that is first suggested by Kimme [12] is applied. In this approach, the special context, that the edge direction on the boundary of a circle is in the direction of its centre, is used. So firstly the local components of the intensity gradient g_x and g_y are calculated. Moreover, the magnitude and the orientation of the local intensity gradient vector are determined by using the following formulas:

$$g=\left(g_x^2+g_y^2\right)^{1/2} \tag{4}$$

$$\theta=\arctan\left(g_y/g_x\right) \tag{5}$$

The centre location coordinates (x_c,y_c) are estimated by:

$$\begin{aligned} x_c &= x-R\cos\theta \\ y_c &= y-R\sin\theta \end{aligned} \tag{6}$$

This method is very robust. In the case that a part of the boundary of an object is obscured or distorted, the object centre can still be found accurately (Figure 4). The irregular broken boundary of the rotating object does not give a suitable centre position. But of only one circular part of the boundary is visible, the true centre point of the rotating object can be determined.

Depending on the image and the parameter setting, the parameter space (accumulation array) has different noise levels and noise frequencies. For suppressing the dominant noise frequency a filter to smooth the accumulation array is applied. If the shapes of the raw image are not very good circles, the accumulation array is a kind of 'stumpy' and will not have a sharp peak. To extract the peak positions in this situation, a filter is used for the search of peaks.

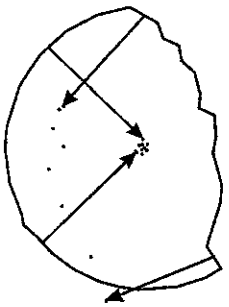

Figure 4: Robustness of the Hough transform

After fitting of circle on the rolling element, a polar transformation is applied to the roller. Afterwards, the marker is tracked by the correlation Method [15]. Figure 5 shows the algorithm procedure steps for one image. For measuring the angular speed of the rolling element, this algorithm must be repeated for the whole recorded image sequence.

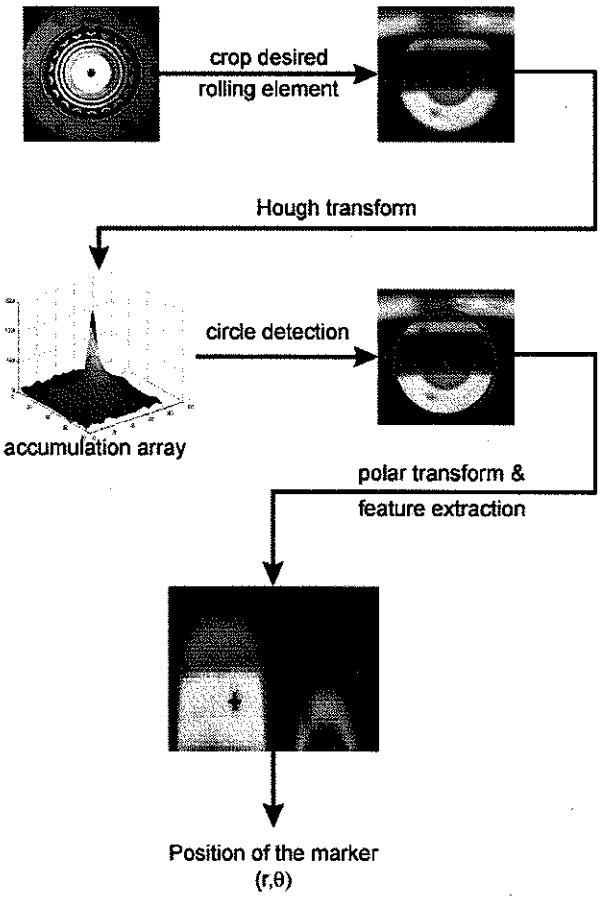

Figure 5: Algorithm procedure for tracking the marker on the rolling element surface

5 EXPERIMENTAL RESULTS

With the above described algorithms the angle of the marker is determined for every image. The time lag between two sequential images is also known. The angular speed of the roller is calculated by:

$$n=\frac{d\theta}{dt} \tag{7}$$

The theoretical rotational speed of the rolling elements is calculated by [16]:

$$n_R = \frac{n_s}{2}\left(\frac{D_p}{D_R} - \frac{\cos^2\alpha}{D_p/D_R}\right) \qquad (7)$$

with:

n_R : rotational speed of the rolling elements, rpm

D_p : pitch diameter = 111.3 mm

D_R : rolling element diameter = 16 mm

α : contact angle = 0°

Figure 6 shows the measured roller slip of the bearing during operation with a shaft rotational speed n_s = 600 rpm of the experimental setup. The value S = 0 means that there is no slip and the roller rotates with the theoretical rotational speed. The value S = 1 indicates the complete sliding of a roller. In this case, the roller has no rotational speed around it's own axis.

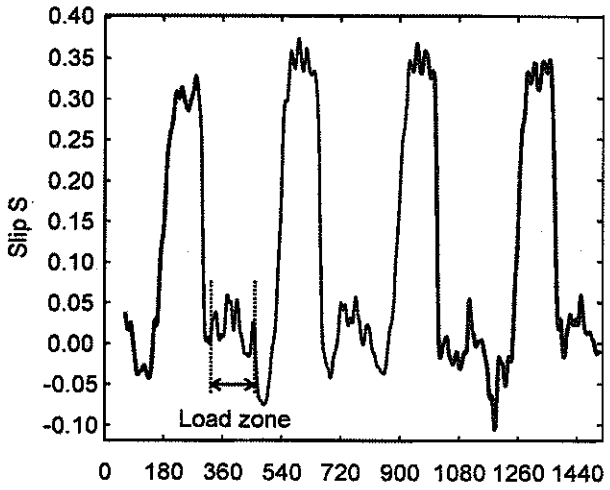

Figure 6: Roller slip during operation with n_s = 600 rpm

Figure 6 shows that there is a maximum slip of about S = 40%. It is a periodic signal. In this experimental setup the loaded zone of the bearing is located at the underneath..

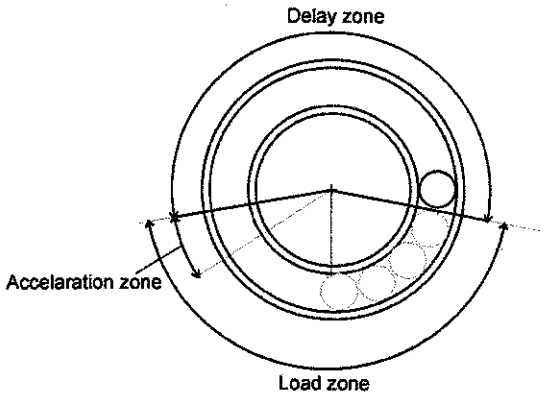

Figure 7: Roller movement during bearing operation

As the roller gets into the load zone of the bearing, no slip occurs. The roller rotates with its theoretical speed. As it comes out of the load zone of the bearing, it slows down (delay zone) and the slip increases at a maximum. Afterwards it accelerates (acceleration zone) till it comes into the load zone again. These 3 zones are principally shown in the Figure 7. For the shaft rotational speed n_s = 200 rpm the maximum slip rise up to S = 100%. In this case, the roller has no rotation and exhibits only slide motion (Figure 8).

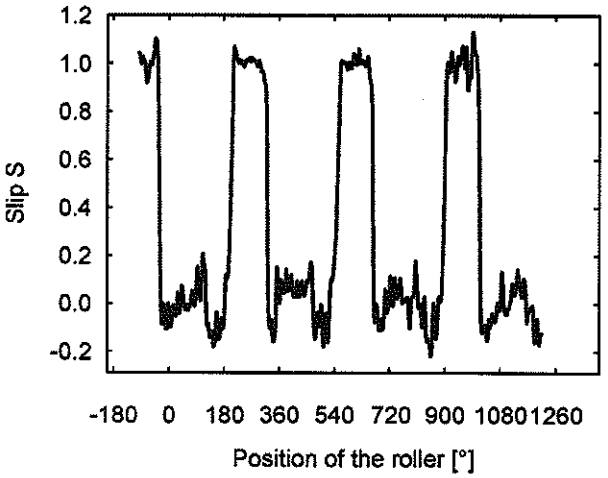

Figure 8: Roller slip during operation with n_s = 200 rpm

Further examinations show, that there is a correlation between the rotational speed of the roller and the slip S. It can be shown, that with increasing roller speed a lower degree of maximum slippage occurs (Figure 9).

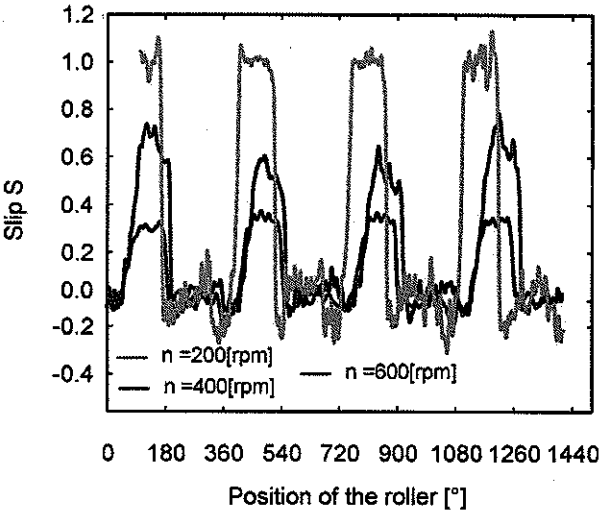

Figure 9: Influence of the shaft rotational speed on the slip S

This knowledge is in contrast to the general opinion [3,9]. That indicates in general more slip of the bearing is caused due to lower loads and higher rotational speeds of the shaft. In the case of the displayed results, comparable low rotational speeds are applied. Further examinations at higher speeds n > 1000 rpm can give more information about the roller behaviour.

6 SUMMARY

In this paper a new method for experimental examination of roller bearing slippage is introduced. The slippage is of interest for technical applications in terms of service life time and preventive failure detection during the bearing operation. The knowledge of the wear enables to protect technical components from malfunction and low productivity. A number of slip measurement methods exists currently. But these methods are constricted to be applied to big-sized bearings. The new slippage measurement enables to measure the slippage of considerable smaller bearings. The main component of this method is a derotator. It allows the stationary view on rotating objects at a wide range of rotational speeds. Furthermore, image processing techniques are applied to extract the movement information of single rollers. The results of experimental investigations of a roller bearing in operation show the principle working of this method. Additionally is shown, that the rotational speed of the bearing influences the degree of roller slip significantly in a range up to n = 600 rpm. Further investigation aim on the effects of slip at rotational speeds greater than 1000 rpm to prove the general assumption of high roller slip at high roller speeds. Additionally, the correlation between the image processing data and the acoustic emissions of the roller bearing will be examined.

7 ACKNOWLEDGMENTS

This work was supported by European Committee as a part of AI4IA (Contract No. 514510) Marie Curie FP6.

The authors would like to thanks support of SKF ERC in the Netherlands, and G. Polll and A. Keßler from IMKT, Leibniz Universität Hannover for their supporting in the realizing the experiments.

8 REFERENCES

[1] Scherb, B., 1997, Zusammenhang zwischen Käfig- und Wälzkörperdrehzahl bei Zylinderrollenlagern, Antriebstechnik 36, 65-69

[2] Wadewitz, M., 1993, Anschmierungserscheinungen; Ursachen der Anschmierung im Wälz-/Gleitkontakt, Forschungsvereinigung Antriebstechnik E.V., Heft 384

[3] Wiemer, M., 1990, Theoretische und experimentelle Untersuchungen zum Betriebsverhalten vollrolliger Zylinderrollenlager, Copy-Team, Hannover

[4] Giese, P., Scherb, B., 1992, Wälzkörpersatzschlupf bei Zylinderrollenlager, Antriebstechnik31, 54-60

[5] Smith, C. F., 1962, Some Aspects of Performance of High-speed Lightly Loaded Cylindrical Roller Bearings, Proc. Ist. n. Mech. Engrs. Vol. 176, Nr. 22

[6] Boness, R. J., 1969, Cage and Roller Slip in High-speed Roller Bearings, Journal Mechanical Engineering Science, Vol. 11, Nr.2, 181-188

[7] Östensen, J. O., 1995, Lubrication of Elastohydrodynamic Contacts Mainly Concerning Low Temperature, Högskolans Tryckeri, Lulea

[8] Wikström, V., Östensen, J.O., Höglund, E., 1990, Friction Torque and Slip of Rollers in Roller Bearings under Arctic Conditions, Proceeding of the 4th Nordic Symp. On Tribology, Lubrication, Friction and Wear, Hirtshals Denmark, 95-103

[9] Tessenow, F., 1973, Theoretische und experimentelle Untersuchungen schnelllaufender Zylinderrollenlager, TU Braunschweig

[10] Davies, E. R., 2005, Machine Vision, Elsevier Inc., 3rd edition

[11] Duda, R. O, Hart, P. E., 1972, Use of the Hough Transform to Detect Lines and Curves in Pictures, Communication of the ACM 15, 11-15

[12] Kimme, C., Ballard, D., Sklancky, J., 1975, Finding circles by an array of accumulators, Communication of ACM 18, 120-122

[13] Atherton, T. J., Kerbyson, D. J., 1999, Size invariant circle detection, Image and vision computing 17, 795-803

[14] Reithmeier, E., Mirzaei, S., Kasyanenko, N., 2008, Optical Vibration and Deviation Measurment of Rotating Machine Parts, Optoelectronics Letters, Vol. 4, No. 1, 45-48

[15] Mirzaei, S., Reithmeier, E., 2007, Digital Image Processing for the Determination of Dynamic Effects in Roller Bearings, 1th. International Conference AI4IA, Ostrava, 51-54

[16] Brändlein, J., 1995, Die Wälzlagerpraxis, Vereinigte Fachverlage